No Effect of Insulin on Glucose Blood-Brain Barrier Transport and Cerebral Metabolism in Humans

Steen G. Hasselbalch, Gitte M. Knudsen, Charlotte Videbaek, Lars Hageman Pinborg, Jes F. Schmidt, Søren Holm, and Olaf B. Paulson

The effect of hyperinsulinemia on glucose blood-brain barrier (BBB) transport and cerebral metabolism (CMR_{glc}) was studied using the intravenous double-indicator method and positron emission tomography using [^{18}F]fluorodeoxyglucose as tracer (PET-FDG). Sixteen normal healthy control subjects (25 ± 4 years old) were studied twice during a euglycemic and a euglycemic-hyperinsulinemic condition. Our hypothesis was that high physiologic levels of insulin did not affect the BBB transport or net metabolism of glucose. During insulin infusion, arterial plasma insulin levels increased from 48.5 to 499.4 pmol/l. The permeability-surface area products for glucose and FDG BBB transport obtained with the double-indicator method remained constant during hyperinsulinemia. Similarly using PET-FDG, no changes were observed in the unidirectional clearance of FDG from blood to brain. k_2* (FDG transport from brain to blood) increased significantly by 15 and 18% (gray and white matter, respectively), and k_4* (dephosphorylation of FDG) increased by 18%. The increase in k_2* may be caused by insulin inducing a decrease in the available FDG brain pool. The increase in k_4* may be related to an increased loss of labeled products during insulin fusion. Irrespective of these changes, CMR_{glc} remained unchanged in all brain regions. We conclude that hyperinsulinemia within the normal physiologic range does not affect BBB glucose transport or net cerebral glucose metabolism. *Diabetes* 48:1915–1921, 1999

Insulin plays a central role in the regulation of carbohydrate metabolism in peripheral tissues, whereas the effect on transport and metabolism of glucose in brain has been much debated. One previous experimental study has suggested that insulin increases glucose transport across the blood-brain barrier (BBB) (1), but most have shown no effect of insulin (2–6). Older studies in humans using high plasma insulin levels (~7,500 pmol/l) have shown an effect of insulin on global glucose transport (7–9). In contrast, in more recent positron emission tomography (PET) studies of diabetic subjects, no effect of insulin on the BBB transport of glucose was found in the control groups (10,11), but in one of these studies, only two control subjects were studied before and during hyperinsulinemia (10); thus data are scarce on the effect of insulin on BBB glucose transport. In line with these studies, PET studies using [^{18}F]fluoro-deoxy-D-glucose (FDG) or methylglucose as tracers have found regional FDG BBB transport to be unaffected by insulin infusion in diabetic men, but no healthy control subjects were studied (12,13).

Studies with regard to the possible effect of insulin on cerebral glucose metabolism (CMR_{glc}) in humans have been conflicting: PET-FDG studies have found no change in CMR_{glc} in healthy (11) or diabetic (13) subjects. Using Fick's principle, Hertz et al. (9) did not observe an effect of very high insulin levels on the global net uptake of glucose, whereas Gottstein and coworkers (7,8) found a 50% increase in net glucose uptake during comparable high levels of plasma insulin.

In the study by Hertz et al. (9), an increase in the unidirectional influx of glucose across the BBB was found when subjects were clamped at very high plasma insulin levels. A reanalysis of that study by means of a mathematical model that takes tracer backflux into account indicates that the increased extraction fraction of glucose was not due to an increased permeability across the BBB, but rather to an increase in the initial distribution volume of the tracer (13a). We have used an intravenous modification of the same method (14) in a group of healthy volunteers to see whether physiologic levels of plasma insulin influence glucose BBB transport. Simultaneous studies with the dynamic PET-FDG method were performed in the same subjects. By combining the two methods, we assessed the glucose transport across the BBB by two independent methods as well as the effect of insulin on regional glucose metabolism. Our hypothesis was that insulin in high physiologic levels did not alter BBB transport or net metabolism of glucose.

RESEARCH DESIGN AND METHODS

Sixteen normal healthy control subjects (age 25 ± 4 years [mean ± SD], range 21–35 years, 11 men, 5 women) were studied. Consent was obtained from each person after written information and explanation of the possible consequences of the study. The study was approved by the Local Ethical Committee of Copenhagen and Frederiksberg County and conducted according to the Helsinki Declaration II.

Each subject was studied twice, during a euglycemic, moderately hypoinsulinemic condition (control study) and during a euglycemic-hyperinsulinemic condition (hyperinsulinemia study). After an overnight fast, including no caffeine, each

From the Neurobiology Research Unit (S.G.H., G.M.K., C.V., L.H.P., O.B.P.), Department of Neurology; Department of Nuclear Medicine (S.H.); and Department of Neuroanesthesiology (J.F.S.), University Hospital, Rigshospitalet, Copenhagen, Denmark.

Address correspondence and reprint requests to Steen G. Hasselbalch, Neurobiology Research Unit N9201, Department of Neurology, University Hospital, Rigshospitalet, Blegdamsvej 9, DK-2100 Copenhagen, Denmark. E-mail: s.hasselbalch@dadlnet.dk.

Received for publication 13 November 1998 and accepted in revised form 7 July 1999.

BBB, blood-brain barrier; CBF, cerebral blood flow; CMR_{glc}, cerebral glucose metabolism; [^{99m}Tc]DTPA, [^{99m}Tc]diethylenetriamine pentaacetic acid; FDG, [^{18}F]fluoro-deoxy-D-glucose; PET, positron emission tomography; ROI, region of interest.

subject was given a standardized light morning meal at 8:30 A.M. No food intake was allowed until the study was completed. Using the Seldinger technique, a catheter was placed in local analgesia (lidocaine 20%) in the internal jugular vein through percutaneous puncture 3 to 4 cm above the clavicle. The correct location of the tip of the catheter was checked by frequent flushing of the catheter followed by the subject's report of a sound close to the ear. In local analgesia (lidocaine 20%), a small catheter was placed in the radial artery in the nondominant hand for arterial blood sampling and in an antecubital vein in both arms, one for injection of radiolabeled isotopes and the other for glucose and insulin infusion.

Two subjects were studied each day. After placement of the catheters, the subjects were randomly allocated to two conditions: one subject was left in the postabsorptive state, whereas a hyperinsulinemic clamp was started in the other. The following week, the order was reversed. Approximately 3 h after start of the clamp, a cerebral blood flow (CBF) study was performed. The subject was then moved to the scanner couch, and immediately a double-indicator study was performed. Half an hour later, a second double-indicator study was performed in combination with the dynamic PET study. The results of the two double-indicator studies were averaged to improve the accuracy of the BBB parameter determination. The hyperglycemia clamp was continued until the end of the PET study.

Hyperinsulinemic-euglycemic clamp. The clamp was started immediately after placement of the catheters. Insulin (Actrapid; Novo Nordisk, Copenhagen) was infused through the indwelling antecubital catheter at a fixed rate of 0.04 IU · m^{-2} surface area · min^{-1}. Five minutes after the start of the insulin infusion, a variable glucose infusion through the same catheter was started. The glucose infusion was increased stepwise from 30 to 120 ml/h over the next hour and adjusted to baseline blood glucose levels by arterial plasma glucose measurements, which were obtained every 5–15 min. A steady-state condition with a constant glucose infusion rate and a constant plasma glucose level was obtained 2–3 h after the clamp start. Arterial plasma glucose was measured with a Beckmann glucose analyzer (Fullerton, CA).

CBF measurement. Global CBF was determined using the 133Xe intravenous injection method and 10 stationary detectors (Cerebrograph 10A; Novo Nordisk) with the subject resting in the supine position. After rapid intravenous injection of 500–600 MBq 133Xe dissolved in 2 ml isotonic saline, the catheter was immediately flushed with 10 ml saline, and CBF was determined by the initial slope index of the semilogarithmically recorded clearance curves (15) and converted to global values as previously described (16). Assuming a constant cerebral rate for oxygen utilization throughout the steady-state clamp condition, as well as during the control condition, CBF was corrected according to changes in the arteriovenous differences of oxygen: $CBF_{BBB} = CBF_{ref} \times (\Delta O_{2(ref)}/\Delta O_{2(BBB)})$, where CBF_{BBB} is CBF at time of double-indicator study, CBF_{ref} is measured CBF, $\Delta O_{2(ref)}$ is arteriovenous difference for oxygen at the time of the CBF measurement, and $\Delta O_{2(BBB)}$ is the arteriovenous oxygen difference at the time of the double-indicator study.

BBB permeability measurements. The basic transport parameters estimated in the present study are PS_1, the permeability surface area product (PS) for transport from blood to brain (ml · g^{-1} · min^{-1}); PS_2, the PS for transport from brain back to blood (ml · g^{-1} · min^{-1}); K_1, the unidirectional clearance from blood to brain (ml · g^{-1} · min^{-1}); k_2, the fractional clearance from brain to blood (g/min); and E_0, the unidirectional extraction fraction (%). Asterisks (*) denote FDG parameters.

The parameters are related in the following way:

$$PS_1 = T_{max}/(K_t + C_c) = -F \times (1 - K_1/F) \quad (1)$$

where T_{max} is the maximal transport rate (μmol · g^{-1} · min^{-1}), K_t is the half-saturation constant (mmol/l), C_c is the capillary glucose concentration, and F is cerebral blood flow (2). K_1 is related, but not identical, to PS_1, and K_1 is lower than PS_1 for substrates with a high extraction across the BBB. For glucose, which has an extraction fraction of about 0.15, the underestimation is approximately 8%. For FDG, which has an extraction fraction of about 0.10, the difference between K_1* and PS_1* is even less. However, when the brain uptake of FDG (and glucose) is compared between the two methods employed in the present study, it is important to take into account methodological differences, discussed below. For FDG transport from brain back to blood, k_2* is the clearance K_2* (corresponding to K_1*) divided by the tracer distribution volume in brain (V_d*). It has the same unit of measure as PS_2*/V_e estimated with the double-indicator method (min^{-1}), but with an important difference in the distribution volumes: V_d* reflects the tracer distribution volume obtained in a 45- to 60-min FDG study, in which the tracer distributes in total brain water, whereas V_e is the tracer distribution volume following a single passage through the capillary bed, and corresponds to the brain interstitial fluid volume (17).

The intravenous double-indicator method, developed in our laboratory (14), was used for estimation of BBB transfer variables. A 5–10 ml bolus containing the tracer compounds was injected intravenously through the antecubital catheter and the catheter was immediately flushed with ~10 ml saline. The bolus contained two test substances: 7 MBq [^{3}H]D-glucose and FDG labeled with either 1.8 MBq ^{14}C or 180–200 MBq ^{18}F and the following reference substances: 7.4 MBq $^{24}Na^+$, 40 MBq [^{99m}Tc]diethylenetriamine pentaacetic acid ([^{99m}Tc]DTPA), and 0.4 MBq $^{36}Cl^-$. $^{24}Na^+$ was obtained from Risø, Denmark. [^{99m}Tc]DTPA, $^{36}Cl^-$, [^{14}C]FDG, and [^{3}H]D-glucose were obtained from Amersham (Arlington Heights, IL). FDG was obtained from Kernforschungsanlage (Jülich, Germany) (specific activity 20 GBq/mg FDG and radiochemical purity >96%). To match test and reference substances with regard to interlaminar diffusion and erythrocyte carriage, a weighted reference curve was calculated: $^{36}Cl^- + 0.5A([^{99m}Tc]DTPA - {}^{24}Na^+) + 0.5A(^{36}Cl^- - {}^{24}Na^+)$ (14). All arterial and venous curves were normalized by dividing the count rate in each sample by the count rate in the standard solution.

Starting 2–3 s before injection, 1-ml blood samples were continuously collected from the radial artery and jugular vein for 50 s by means of a sampling machine (Ole Dich Instrumentmakers, Hvidovre, Denmark) at a fixed interval of 1.3 s. Blood samples were immediately placed on ice and centrifuged, and plasma was taken for counting in a gamma counter (Packard Autogamma 5385; Packard Instruments, Downers Grove, IL). Corrections for background, spillover, and decay were applied. After at least 3 weeks, 3 ml scintillation fluid (Picofluor 40; Packard) was added and beta-emitting isotopes were counted (PA 800-CA; Packard) with corrections for quenching and spillover using the method of external standardization.

To correct for differences in the brain input of test and reference substances, a five-parameter Dirac impulse response for passage through the cerebrovascular bed was computed from the input and output of the reference substance. This response was then combined with the single membrane (well-mixed) model of the brain, which treats the endothelial luminal and abluminal membranes as a single membrane (17). Convolving the impulse response with the arterial input curve of the test substance yields a theoretical test output curve, which is iteratively compared to the actual test output curve. When CBF is known, the values of the model variables and the standard errors of the estimates giving the best fit between theory and observation can be obtained by minimizing the sum of squares of the differences between the theoretical and the measured outflow test curve using the simplex method. The BBB glucose transport was estimated by PS_1 and PS_2/V_e and FDG transport by PS_1* and PS_2*/V_e. To calculate PS_2 and PS_2*, a fixed value of 0.15 ml/g was assigned for V_e based on previous findings, where glucose distributed in a volume corresponding to the brain interstitial space (17). E_0 and E_0*, the average unidirectional extraction fractions for glucose and FDG (%), were estimated as separate parameters, and finally, unidirectional glucose influx from blood to brain was calculated as $PS_1 \times C_c$, where C_c, the capillary tracer concentration, was calculated as the average of the arterial and venous plasma glucose concentrations. It was assumed that the intravenously injected bolus mixed completely with blood before arrival at the brain capillaries so that systemically measured arterial blood substrate concentrations equaled those of the brain capillaries. This assumption was secured by the finding that blood glucose concentrations in blood samples from four subjects before the bolus activity peak, at maximum of activity, and after the bolus peak remained constant (S.G.H., G.M.K., J. Jakobsen, L.H.P., O.B.P., unpublished observations).

PET-FDG. Dynamic PET scanning was performed with the Therascan 3128 PET camera (Atomic Energy of Canada, Ottawa, Ontario, Canada). An individual head holder was molded for each person by filling a two-component plastic foam into a perspex semicylinder; the holder was used for both study days. Three consecutive 12-mm slices with an image plane resolution of 20 mm were obtained. Slices were placed 48, 50, and 62 mm above the canthometal line (+CM; a line through the lateral canthus of the eye and the outer meatus of the ear). Two different scan setups were used to evaluate the effect of prolonging the scan time on estimation of the transfer coefficients. Twelve subjects were studied using a short, low time resolution setup (0–10 min, 1-min scans; 10–20 min, 2-min scans; and 20–45 min, 5-min scans). Four subjects were studied using a long, high resolution study setup (0–1 min, 6-s scans; 1–2 min, 20-s scans; 2–10 min, 1-min scans; 10–20 min, 2-min scans; 20–45 min, 5-min scans; and 45–95 min, 10-min scans). A second double-indicator measurement with 180–200 MBq FDG added to the bolus was performed simultaneously with the dynamic PET scanning. After rapid intravenous injection of the bolus in 5–10 ml saline, 1-ml blood samples were drawn from the radial artery every 1.3 s from time 0 to 50 s, followed by manual sampling with increasing time intervals for the rest of the PET study. Corrections for dead time, attenuation, and scatter were performed as previously described (18). Calibration of the PET camera and cross-calibration between the PET camera and the gamma counter were performed at the end of each study day.

Thirty circular regions of interest (ROIs) with a diameter of 20 mm were placed on the cortical rim of the three slices. An individual ROI template, drawn for each slice, was used to ensure the same position of ROIs in control and insulin studies. Two to six ROIs were placed in periventricular white matter at the level of 62 mm +CM. ROIs were averaged into four groups: frontal cortex, temporal cortex, occipital cortex, and white matter. Since preliminary analysis did not reveal any significant side difference, corresponding left and right hemisphere ROIs were averaged.

Determination of FDG transfer coefficients, CMR_{glc}, and the lumped constant. Transfer coefficients for FDG (K_1*, unidirectional plasma clearance [ml · g^{-1} · min^{-1}], k_2*, fractional brain-blood clearance [g/min], and k_3*, fractional

phosphorylation rate of FDG to FDG-6-phosphate [g/min]) were estimated from the time-activity curves in arterial plasma and brain for each individual ROI using the autoradiographic method adapted for studies in humans (19). In all 16 subjects, dephosphorylation of FDG-6-phosphate was either assumed to be negligible ($k_4^* = 0$, not included in the fitting procedure, 3K model) or included (4K model) as described by Huang et al. (20). Activity in the vascular compartment was subtracted from the total brain activity after the plasma volume (V_p) had been fitted as an additional parameter in each region. Correction for delay between blood and brain activity was applied by observing the time difference between the bolus peak coincidence number on the scanner control panel and the bolus peak activity in the blood samples.

CMR_{glc} was calculated from the equation

$$CMR_{glc} = (C_a/LC) \times ([K_1^* \times k_3^*]/[k_2^* + k_3^*]) \quad (2)$$

where C_a is plasma glucose concentration, LC is the lumped constant, which corrects for differences in glucose and FDG BBB transport and phosphorylation, and K_1^*, k_2^*, and k_3^* are the transfer coefficients mentioned above (20).

The lumped constant, LC, was experimentally determined from the transfer coefficients obtained by dynamic PET (21) by the equation

$$LC = (k_3^*/k_3) + ([K_1^*/K_1] - [k_3^*/k_3]) \times (K^*/K_1^*) \quad (3)$$

where k_3^*/k_3, the ratio of phosphorylation between FDG and glucose, equals 0.38 (22); K_1^*/K_1, the ratio between FDG and glucose unidirectional clearances, is 1.48 (23); and K^* is net clearance of FDG = $(K_1^* \times k_3^*)/(k_2^* + k_3^*)$.

Blood samples. On both study days, plasma insulin and glucose levels in arterial plasma were measured before the CBF measurement, before each of the double-indicator measurements, and four times during the PET scanning. During the hyperinsulinemic clamp, arterial plasma glucose level was measured when required, usually every 10–15 min. Hematocrit, hemoglobin, sodium, and potassium were measured at the end of each study. Arteriovenous differences for oxygen and carbon dioxide were obtained before CBF and the double-indicator measurements (ABL-30; Radiometer, Copenhagen).

Statistics. The null-hypothesis of no change in BBB transport or metabolism of glucose was tested using Student's paired t test between control and insulin studies. A P value of less than 5% was considered significant.

RESULTS

During the hyperinsulinemic clamp, arterial plasma insulin levels increased 10-fold from a mean control value of 48.5 pmol/l to 499.4 pmol/l, whereas plasma glucose remained constant at normoglycemic values (Tables 1 and 2; Fig. 1*A* and *B*). As expected, insulin caused a small decrease in plasma potassium concentration. Global CBF remained constant (0.45 ± 0.06 vs. 0.48 ± 0.05) (Table 3).

BBB transport parameters for D-glucose measured with the double-indicator technique are shown in Table 4. PS_1, PS_2, or their ratio did not change during insulin infusion. Likewise, the unidirectional extraction fraction (E_0) remained constant at 15.6%. As a consequence of the unchanged permeability, no changes were observed in the unidirectional influx of glucose ($PS_1 \times C_a$). In accordance with the unchanged transport parameters for glucose, no changes in BBB parameters for FDG were found, and the ratio between the unidirectional clearance for FDG and glucose also remained unchanged (Table 4).

TABLE 1
Arterial plasma levels of measured substances during control and hyperinsulinemic clamp studies

	Control	Hyperinsulinemia
Glucose (mmol/l)	5.13 ± 0.41	5.19 ± 0.43
Insulin (pmol/l)	48.5 ± 16.7	499.4 ± 90.6*
Hematocrit (%)	40.2 ± 2.7	39.2 ± 3.1
Sodium (mmol/l)	141.8 ± 3.3	142.1 ± 1.8
Potassium (mmol/l)	3.9 ± 0.8	3.3 ± 0.4*

Data are means ± SD. *$P < 0.002$, Student's matched-pairs t test.

TABLE 2
Hemoglobin and hematocrit levels before and after clamp studies (both control and hyperinsulinemia)

	Before	After
Hemoglobin (mmol/l)	8.5 ± 0.5	8.4 ± 0.7
Hematocrit (%)	40.3 ± 3.0	39.6 ± 2.9*

Data are means ± SD. *$P < 0.01$, Student's matched-pairs t test.

The regional transfer coefficients measured by PET are shown in Table 5. No changes were observed in the unidirectional clearance (K_1^*) or in the phosphorylation (k_3^*) of FDG. The transport of FDG from brain back to blood (k_2^*) increased significantly by 15% in mean gray matter and by 18% in white matter during insulin infusion, compatible with a

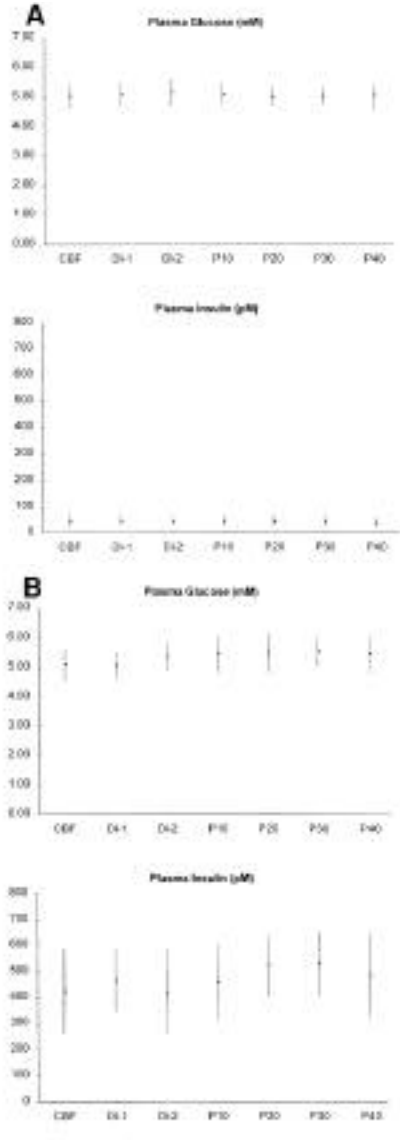

FIG. 1. Plasma glucose and insulin concentrations. Values are means (dots) and 1 SD below and above mean (vertical lines). *A*: Control study. *B*: Hyperinsulinemic study. DI-1, 1st double-indicator measurement; DI-2, 2nd double-indicator measurement; P10–P40, PET-FDG study at 10–40 min.

TABLE 3
CBF, pH, and Pa_{CO_2} during control and hyperinsulinemic clamp studies

	Control	Hyperinsulinemia
n	16	16
CBF_{global} (ml · g^{-1} · min^{-1})	0.45 ± 0.06	0.48 ± 0.05
pH	7.40 ± 0.01	7.40 ± 0.02
Pa_{CO_2} (kPa)	5.07 ± 0.26	4.98 ± 0.39

Data are means ± SD. CBF_{global}, global cerebral blood flow; Pa_{CO_2}, partial pressure of CO_2 in arterial blood. All values NS ($P > 0.05$), Student's matched-pairs *t* test.

small (not significant) decrease in the brain/blood distribution volume of FDG (V_d) and a concomitant decrease in LC. The lack of significant increase in k_2* in occipital cortex was probably due to the small number of ROIs included in this region. CMR_{glc} remained constant in all regions with no significant regional differences in the gray matter response to insulin infusion. Therefore, in the further analysis of the PET-FDG results, only data from mean gray matter and white matter were considered. Inclusion of dephosphorylation of FDG-6-phosphate (k_4*) in the PET-FDG model yielded similar results to those obtained with the 3K model: there was a significant increase in mean gray matter k_2*, whereas K_1* and k_3* were unchanged (Table 6). Interestingly, insulin infusion was accompanied by an increase in k_4* of 18% in both gray and white matter, but it did not affect CMR_{glc}, which—in accordance with the 3K model—remained constant during hyperinsulinemia.

In the four subjects scanned for 95 min, in both conditions, k_4* was 30–33% smaller in both gray and white matter compared with the 12 subjects scanned for 45 min, whereas no changes in the other transfer coefficients or in CMR_{glc} were observed (data not shown).

The effect of insulin on the FDG time-activity curves is shown in Fig. 2. Insulin infusion caused a considerable decrease in the area under the arterial FDG curve, resulting in a corresponding rapid change in the brain FDG activity curve. During insulin infusion, the FDG activity in brain reached a maximum at 8 min, and thereafter a slight but significant decrease in brain activity was noted. At 45 min, the brain FDG activity was 92% of the peak activity; after 95 min, the activity was further reduced to 82% of the peak activity.

TABLE 4
BBB permeability surface area, extraction fraction, and unidirectional influx for D-glucose and FDG measured by intravenous double-indicator method during control and hyperinsulinemic clamp studies

	Control	Hyperinsulinemia
D-glucose		
PS_1 (ml · g^{-1} · min^{-1})	0.077 ± 0.018	0.081 ± 0.031
PS_2 (ml · g^{-1} · min^{-1})	0.126 ± 0.087	0.125 ± 0.076
PS_2/PS_1	1.65 ± 1.0	1.91 ± 2.06
E_0 (%)	15.6 ± 3.6	15.1 ± 4.2
K_1 (ml · g^{-1} · min^{-1})	0.070 ± 0.018	0.072 ± 0.025
Influx (μmol · g^{-1} · min^{-1})	0.395 ± 0.115	0.423 ± 0.162
FDG		
PS_1* (ml · g^{-1} · min^{-1})	0.115 ± 0.029	0.118 ± 0.034
PS_2* (ml · g^{-1} · min^{-1})	0.106 ± 0.060	0.149 ± 0.105
PS_2*/PS_1*	0.94 ± 0.52	1.17 ± 1.01
E_0* (%)	22.7 ± 4.8	21.6 ± 4.7
K_1* (ml · g^{-1} · min^{-1})	0.101 ± 0.023	0.099 ± 0.037
K_1*/K_1 (ratio)	1.49 ± 0.23	1.55 ± 0.33

Data are means ± SD. PS_1, permeability surface area for transport from blood to brain; PS_2, permeability surface area for transport from brain to blood; E_0= extraction fraction in percent; K_1, unidirectional clearance equal to CBF × E_0; influx, unidirectional influx from blood to brain calculated from $PS_1 \times C_a$, where C_a is arterial plasma concentration of glucose.

DISCUSSION

The present study showed no changes in the BBB transport of FDG and glucose during physiologic hyperinsulinemia. Further, although we found evidence for a change in the metabolism of FDG, neither regional nor global changes were found in net cerebral glucose metabolism, and global cerebral blood flow also remained constant.

Plasma insulin levels. In the present study, the plasma insulin level was intentionally kept within normal physiologic range: during insulin infusion, mean plasma insulin concentration increased to 500 pmol/l, which is comparable to a previously obtained postprandial mean value of 350 pmol/l following ingestion of a normal meal (24). The insulin infusion created a marked effect on the FDG activity curves (Fig. 2), most likely because of a rapid plasma clearance due to the insulin-dependent increase in FDG uptake by muscle tissue (24). The clearance to peripheral tissue was also evident from the amount of infused glucose required to maintain normoglycemia (typically 200 mmol/h). In conclusion, the insulin concentration in the present study was sufficiently elevated to high, but physiologically relevant, levels.

BBB permeability measurements. Two independent methods were used in the present study to evaluate the effect of insulin per se on glucose BBB transport, and no changes in glucose or FDG uptake were found. With both methods, the most consistent finding was a constant unidirectional clearance of FDG and glucose from blood to brain (K_1* and K_1). There were substantial differences, however, in the absolute values obtained with the two methods: global K_1* estimated from the PET data in Table 5 was lower than K_1* obtained from the double-indicator method (0.089 ± 0.013 vs. 0.101 ± 0.023; NS). Methodological differences most likely explain the discrepancy: the double-indicator method has a high time-resolution with a short experimental time and estimates K_1* during a single passage of the tracer through the cerebrovascular bed in contrast to PET-FDG, which predominantly determines K_1* from the first minutes of the time-activity curves. During the longer measurement time with PET-FDG, BBB parameter estimation is influenced by several factors, among which tissue heterogeneity is important (25). When this factor is incorporated into the model, the estimate of K_1* increases, reflecting that the conventional 3K model underestimates tracer backflux (k_2*) and consequently K_1* (25). In theory, the double-indicator method may yield more physiologically meaningful BBB transport parameters, but with a greater variation than those obtained with PET (Tables 4 and 5). Taking into account the variation in the double-indicator BBB parameter estimations, the possibility of a type 2 error must be considered. We could not exclude increases in unidirectional extraction and influx of less than

TABLE 5
Regional transfer coefficients for FDG and cerebral glucose metabolism measured by PET-FDG during control and hyperinsulinemic clamp studies

ROI	K_1* (ml · g^{-1} · min^{-1})	k_2* (g/min)	k_3* (g/min)	V_p fraction	V_d* (ml/g)	K* (ml · g^{-1} · min^{-1})	LC (ratio)	CMR_{glc} (ml · g^{-1} · min^{-1})
Control								
Frontal	0.098 ± 0.014	0.102 ± 0.024	0.066 ± 0.013	0.041 ± 0.011	0.594 ± 0.114	0.038 ± 0.005	0.818 ± 0.063	0.241 ± 0.034
Temporal	0.102 ± 0.016	0.110 ± 0.027	0.012 ± 0.012	0.044 ± 0.011	0.588 ± 0.102	0.038 ± 0.006	0.797 ± 0.068	0.244 ± 0.034
Occipital	0.124 ± 0.026	0.143 ± 0.043	0.067 ± 0.010	0.048 ± 0.014	0.602 ± 0.132	0.039 ± 0.005	0.743 ± 0.087	0.273 ± 0.047
Mean gray matter	0.103 ± 0.015	0.111 ± 0.025	0.066 ± 0.011	0.043 ± 0.010	0.594 ± 0.098	0.039 ± 0.005	0.800 ± 0.065	0.247 ± 0.033
White matter	0.067 ± 0.010	0.096 ± 0.021	0.051 ± 0.011	0.024 ± 0.007	0.459 ± 0.077	0.024 ± 0.003	0.774 ± 0.054	0.157 ± 0.023
Global	0.089 ± 0.013	0.099 ± 0.021	0.061 ± 0.010	0.035 ± 0.008	0.562 ± 0.100	0.033 ± 0.004	0.808 ± 0.057	0.206 ± 0.027
Insulin								
Frontal	0.098 ± 0.010	0.120 ± 0.022*	0.064 ± 0.009	0.039 ± 0.015	0.540 ± 0.096	0.034 ± 0.007	0.766 ± 0.056*	0.229 ± 0.024
Temporal	0.103 ± 0.013	0.129 ± 0.018*	0.065 ± 0.010	0.043 ± 0.016	0.534 ± 0.089	0.035 ± 0.007	0.751 ± 0.058*	0.237 ± 0.029
Occipital	0.121 ± 0.019	0.156 ± 0.036	0.066 ± 0.010	0.048 ± 0.022	0.561 ± 0.133	0.037 ± 0.008	0.717 ± 0.067	0.264 ± 0.041
Mean gray matter	0.103 ± 0.010	0.128 ± 0.021*	0.065 ± 0.009	0.042 ± 0.022	0.542 ± 0.089	0.035 ± 0.007	0.754 ± 0.056*	0.231 ± 0.023
White matter	0.068 ± 0.009	0.113 ± 0.020*	0.051 ± 0.011	0.024 ± 0.009	0.416 ± 0.052	0.021 ± 0.004*	0.722 ± 0.041†	0.150 ± 0.018
Global	0.089 ± 0.009	0.122 ± 0.017*	0.059 ± 0.009	0.034 ± 0.013	0.493 ± 0.065*	0.029 ± 0.005	0.761 ± 0.047†	0.197 ± 0.190

Data are means ± SD. K_1*, k_2*, and k_3* are transfer coefficients for transport and phosphorylation of FDG as described in METHODS; V_p is plasma volume in brain; V_d* is the distribution volume of FDG in brain; K* is net clearance of FDG calculated as $(K_1 * k_3*)/(k_2* + k_3*)$; LC is the FDG lumped constant (for calculation, see Eq. 3); CMR_{glc} is cerebral glucose metabolism calculated as C_pK*/LC, where C_p is plasma glucose concentration; global, global values calculated from mean gray and white matter values assuming a gray:white matter ratio of 60:40. *$P < 0.05$, †$P < 0.01$, Student's t test for matched pairs.

25–30% with a 5% significance level, but when comparing this theoretical increase with the PET-FDG results, it is unlikely to have taken place: the smaller variation of the PET-FDG method allowed increases in K_1* of >8 and >10% (in gray and white matter, respectively) to be detected, and these were not observed.

In a previous study from our group using the intracarotid double-indicator method without correcting for tracer backflux and capillary heterogeneity, unidirectional influx of glucose increased by 45% and the extraction fraction by 14–21% during hyperinsulinemia (9). The double-indicator method has since been modified in several ways: a model that takes into account tracer backflux from brain to blood and capillary heterogeneity was introduced (17), and recently, the method was adapted for intravenous injection of the BBB tracers (14), allowing for studies in humans without carotid puncture. Applying the mathematical model with estimation of tracer backflux used in the present study on the data by Hertz et al. (9), the apparent increase in PS_1 was not caused by an increased transport capacity, but rather by a significant decrease in PS_2/V_e (13a). This decrease was explained by an increase in the initial distribution volume of glucose (V_e) secondary to an increased transport of glucose from the brain interstitial fluid into the intracellular compartment. These findings are in agreement with the present study, where PS_1 remained constant, suggesting that, even in very high doses, insulin does not alter the brain uptake of glucose.

In a comprehensive experimental setup using autoradiography and labeled methyl-glucose in rats, Namba et al. (6) found a subtle *decrease* in glucose transport during insulin

TABLE 6
Transfer coefficients for FDG and cerebral glucose metabolism in gray and white matter during hyperinsulinemia estimated by PET-FDG using the 4K model

ROI	K_1* (ml · g^{-1} · min^{-1})	k_2* (g/min)	k_3* (g/min)	k_4* (g/min)	V_p fraction	V_d (ml/g)	K* (ml · g^{-1} · min^{-1})	LC (ratio)	CMR_{glc} (ml · g^{-1} min^{-1})
Control									
Mean gray matter	0.121 ± 0.014	0.197 ± 0.031	0.126 ± 0.028	0.011 ± 0.004	0.031 ± 0.017	0.383 ± 0.071	0.047 ± 0.007	0.810 ± 0.049	0.295 ± 0.037
Mean white matter	0.074 ± 0.013	0.142 ± 0.040	0.093 ± 0.025	0.011 ± 0.005	0.018 ± 0.007	0.324 ± 0.060	0.029 ± 0.004	0.817 ± 0.057	0.182 ± 0.027
Hyperinsulinemia									
Mean gray matter	0.121 ± 0.020	0.224 ± 0.040*	0.124 ± 0.022	0.013 ± 0.003*	0.033 ± 0.017	0.348 ± 0.047	0.043 ± 0.009	0.777 ± 0.049	0.286 ± 0.043
Mean white matter	0.073 ± 0.010	0.162 ± 0.028	0.092 ± 0.019	0.013 ± 0.005†	0.022 ± 0.011	0.295 ± 0.051	0.027 ± 0.005	0.779 ± 0.033*	0.176 ± 0.020

Data are means ± SD. See Table 3 for abbreviations. *$P < 0.05$, †$P < 0.01$, Student's t test for matched pairs.

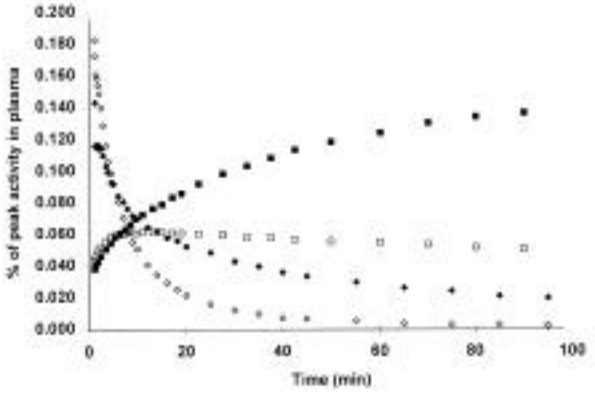

FIG. 2. FDG time-activity curves in plasma and brain (mean gray matter). Plasma FDG activity during normoinsulinemia (◆) and hyperinsulinemia (◇); brain FDG activity during normoinsulinemia (■) and hyperinsulinemia (□). Values are means of four subjects scanned from 0–95 min (% of maximal plasma activity). Note the rapid plasma clearance of FDG during insulin infusion with concomitant change in brain FDG activity. During insulin infusion, a decline in the brain FDG activity was noted, indicating a loss of label.

infusion. In contrast, using a modified deoxyglucose method, Hom et al. (4) did not demonstrate any changes in the brain uptake of glucose during hyperinsulinemia, but in that study the unidirectional glucose influx was not measured. In other studies, methodological problems also render the interpretation of the results difficult: the findings of an increased transport capacity in rats (1) and humans (7,8) may be explained by the lack of glucose steady-state conditions in those studies. Following an increase in plasma glucose, influx of glucose is increased and studies carried out before a new steady state has been reached between brain glucose and plasma glucose concentrations overestimate glucose influx. PET studies during hyperinsulinemia in healthy humans are scarce. In a PET-FDG study in nine volunteers, Shapiro et al. (11) confirmed the negative findings in rats with no change in K_1* during insulin infusion. Other negative studies have included too few subjects to draw any firm conclusions (10,12).

The finding of an insulin-insensitive BBB glucose transport is consistent with the finding that the predominant glucose transporter in brain endothelium is the insulin-insensitive isoform GLUT1, whereas the insulin-sensitive isoform GLUT4 is almost solely expressed in adipocytes and muscle cells (26). A recent experimental study, however, indicated that GLUT4 is present in some structures in the brain, including cerebellum (27). Since we did not include cerebellum in the FDG ROI analysis, we cannot determine whether insulin changed the FDG transfer coefficients in this region and can only conclude from the double-indicator data that possible changes in cerebellum transport rates were too small to affect the global BBB parameters.

Whereas the double-indicator method did not reveal any changes in the FDG transport from brain back to blood (PS_2), dynamic PET showed a significant increase in this transport (k_2*). The variation in PS_2* (and PS_2) was much higher than the variation in k_2*, and an increase in PS_2 may have been obscured by this variation. The exact physiologic significance of a possible increase in k_2* (or PS_2*) is difficult to evaluate: they both incorporate the outward BBB tracer transport as well as the brain distribution volume of the tracer. The k_2* increase during insulin infusion may thus reflect an increase in BBB transport parameters (T_{max}, K_t) from brain to blood or a change in the tracer distribution volume. Because BBB glucose transport occurs through a transmembrane transporter and the inward transport (K_1*) did not change, it is not likely that T_{max}, which reflects the maximal number of transporters, increased during insulin infusion. In theory, however, the affinity (K_t) to the abluminal transporter may selectively have increased, but the most likely explanation for the k_2* increase is a decrease in the distribution volume of FDG in the brain, representing a decrease in free FDG (and glucose) concentration in the brain. This could be induced by an increased metabolism of FDG or by transfer of FDG into other compartments. During the experimental time of 45–60 min, insulin presumably had penetrated the BBB (28) and could have promoted anabolic pathways such as increasing glycogen deposits (29). Although all these pathways should be reflected in an increase in k_3*, a type 2 error could have obscured changes in k_3*; even though we have no evidence to support this hypothesis, it remains the most plausible. In conclusion, the increase in k_2* remains unexplained, but may reflect a decrease in the free brain FDG concentration due to an insulin effect on the metabolism of FDG beyond the BBB.

Determination of regional glucose metabolism. Regional cerebral glucose metabolism measured by PET-FDG did not change during insulin infusion in any of the regions studied, in accordance with the negative findings obtained in rats (30), healthy human subjects (11), and diabetic subjects (13). In an autoradiographic study in rats, Lucignani et al. (31) found small regional increases in CMR_{glc} in certain hypothalamic nuclei. The spatial resolution of our PET camera, however, did not allow us to reach conclusions on insulin effects on CMR_{glc} in subcortical gray matter structures.

The correct determination of the glucose metabolism from PET-FDG requires knowledge of the ratio between FDG and glucose net uptake, expressed as the lumped constant. The calculation of the lumped constant (Eq. 3) assumes constant ratios between FDG and glucose transfer coefficients, and this assumption was verified for the K_1*/K_1 ratio (Table 4). The mean K_1*/K_1 ratio of 1.55 was comparable to previously obtained values during normo-, hypo-, and hyperglycemia ranging from 1.41 to 1.48 (32), suggesting that the transfer coefficient ratio remains unchanged in hyperinsulinemia. Most variations in the lumped constant are caused by variations in the distribution volumes of FDG and glucose that occur during changes in plasma glucose levels (33). In the present study, the decrease in the distribution volume ratio between FDG and glucose caused a decrease in the lumped constant (Tables 5 and 6). Because there exists an inverse linear relationship between LC and CMR_{glc}, the estimation of LC is important in quantitative PET-FDG, and it is suggested that concomitant determination of the lumped constant improves the accuracy of the CMR_{glc} calculation in situations that may cause changes in the distribution volumes of FDG and glucose (hypo- and hyperglycemia and hyperinsulinemia).

In accordance with a previous study showing that transfer coefficients decrease with experimental time (25), the parameter for product loss (k_4*, usually ascribed to dephosphorylation of FDG-6-phosphate) was significantly lower in the four subjects scanned for 95 min compared with the 12 subjects scanned for 45 min. Interestingly, in their PET-FDG study, Eastman et al. (10) found the same increase in k_4* dur-

ing insulin infusion that we observe in the present study. Figure 1 illustrates that during insulin infusion, significant product loss was observed. Therefore, our data imply that insulin infusion resulted in an increased loss from brain of FDG or labeled metabolites, and the nature of this loss needs to be determined more precisely.

We conclude that insulin does not affect BBB transport or the overall level of CMR_{glc} in the human brain, but that insulin may alter brain glucose metabolism by affecting the compartmentalization or further metabolism of glucose in a yet unresolved manner.

REFERENCES

1. Daniel PM, Love ER, Pratt OE: Insulin and the way the brain handles glucose. *J Neurochem* 25:471–476, 1975
2. Crone C: Facilitated transfer of glucose from blood into brain tissue. *J Physiol* 181:103–113, 1965
3. Betz AL, Gilboe DD, Yudilevich DL, Drewes LR: Kinetics of unidirectional glucose transport into the isolated dog brain. *Am J Physiol* 225:586–592, 1973
4. Hom FG, Goodner CJ, Berrie MA: A [^{3}H]2-deoxyglucose method for comparing rates of glucose metabolism and insulin responses among rat tissues in vivo: validation of the model and the absence of an insulin effect on brain. *Diabetes* 33:141–152, 1984
5. McCall AL, Gould JB, Ruderman NB: Diabetes-induced alterations of glucose metabolism in rat cerebral microvessels. *Am J Physiol* 247:E462–E467, 1984
6. Namba H, Lucignani G, Nehlig A, Patlak C, Pettigrew K, Kennedy C, Sokoloff L: Effects of insulin on hexose transport across blood-brain barrier in normoglycemia. *Am J Physiol* 252:E299–E303, 1987
7. Gottstein U, Held K, Sebening H, Walpurger G: Glucose consumption of the human brain under the influence of intravenous infusions of glucose, glucagon and glucose-insulin. *Klin Wochenschr* 43:965–975, 1965 [in German]
8. Gottstein U: The effect of insulin on cerebral glucose uptake in normal and diabetic human subjects. In *Brain Work*. Ingvar DH, Lassen NA, Eds. Copenhagen, Munksgaard, 1975, p. 144–148
9. Hertz MM, Paulson OB, Barry DI, Christiansen JS, Svendsen PA: Insulin increases glucose transfer across the blood-brain barrier in man. *J Clin Invest* 67:597–604, 1981
10. Eastman RC, Carson RE, Gordon MR, Berg GW, Lillioja S, Larson SM, Roth J: Brain glucose metabolism in noninsulin-dependent diabetes mellitus: a study in Pima Indians using positron emission tomography during hyperinsulinemia with euglycemic glucose clamp. *J Clin Endocrinol Metab* 71:1602–1610, 1990
11. Shapiro ET, Cooper M, Chen CT, Giwen BD, Polonsky KS: Change in hexose distribution volume and fractional utilization of [18-F]-2-deoxy-2-fluoro-D-glucose in brain during acute hypoglycemia in humans. *Diabetes* 39:175–180, 1990
12. Brooks DJ, Gibbs JS, Sharp P, Herold S, Turton DR, Luthra SK, Kohner EM, Bloom SR, Jones T: Regional cerebral glucose transport in insulin-dependent diabetic patients studied using [^{11}C]3-*O*-methyl-D-glucose and positron emission tomography. *J Cereb Blood Flow Metab* 6:240–244, 1986
13. Cranston I, Marsden P, Matyka K, Evans M, Lomas J, Sonksen P, Maisey M, Amiel SA: Regional differences in cerebral blood flow and glucose utilization in diabetic man: the effect of insulin. *J Cereb Blood Flow Metab* 18:130–140, 1998

13a. Knudsen GM, Hasselbalch SG, Hertz MM, Paulson OB: High dose insulin does not increase glucose transfer across the blood-brain barrier in humans: a re-evaluation. Eur J Clin Invest 29:687–691, 1999

14. Knudsen GM: Application of the double-indicator technique for measurement of blood-brain barrier permeability in humans. *Cerebrovasc Brain Metab Rev* 6:1–30, 1994
15. Olesen J, Paulson OB, Lassen NA: Regional cerebral blood flow in man determined by the initial slope of the clearance of intra-arterially injected ^{133}Xe. *Stroke* 2:519–540, 1971
16. Hasselbalch SG, Knudsen GM, Jakobsen J, Hageman LP, Holm S, Paulson OB: Blood-brain barrier permeability of glucose and ketone bodies during short-term starvation in humans. *Am J Physiol* 268:E1161–E1166, 1995
17. Knudsen GM, Pettigrew KD, Paulson OB, Hertz MM, Patlak CS: Kinetic analysis of blood-brain barrier transport of D-glucose in man: quantitative evaluation in the presence of tracer backflux and capillary heterogeneity. *Microvasc Res* 39:28–49, 1990
18. Cooke BE, Evans AC, Fanthome EO, Alerie E, Sendyk AM: Performance figures and images from the Therascan 3128 positron emission tomography. *IEEE Trans Nucl Sci* NS31:640–644, 1984
19. Reivich M, Kuhl D, Wolf A, Greenberg J, Phelps M, Ido T, Casella V, Fowler J, Hoffman E, Alavi A, Som P, Sokoloff L: The [^{18}F]fluorodeoxyglucose method for the measurement of local cerebral glucose utilization in man. *Circ Res* 44:127–137, 1979
20. Huang SC, Phelps ME, Hoffman EJ, Sideris K, Selin CJ, Kuhl DE: Noninvasive determination of local cerebral metabolic rate of glucose in man. *Am J Physiol* 238:E69–E82, 1980
21. Kuwabara H, Evans AC, Gjedde A: Michaelis-Menten constraints improved cerebral glucose metabolism and regional lumped constant measurements with [^{18}F]fluorodeoxyglucose. *J Cereb Blood Flow Metab* 10:180–189, 1990
22. Hasselbalch SG, Madsen PL, Knudsen GM, Holm S, Paulson OB: Calculation of the FDG lumped constant by simultaneous measurements of global glucose and FDG metabolism in humans. *J Cereb Blood Flow Metab* 18:154–160, 1998
23. Frayn KN, Coppack SW, Potts JL: Effect of diet on human adipose tissue metabolism. *Proc Nutr Soc* 51:409–418, 1992
24. Huitink JM, Visser FC, van Leeuwen GR, van Lingen A, Bax JJ, Heine RJ, Teule GJ, Visser CA: Influence of high and low plasma insulin levels on the uptake of fluorine-18 fluorodeoxyglucose in myocardium and femoral muscle, assessed by planar imaging. *Eur J Nucl Med* 22:1141–1148, 1995
25. Schmidt K, Lucignani G, Moresco RM, Rizzo G, Gilardi MC, Messa C, Colombo F, Fazio F, Sokoloff L: Errors introduced by tissue heterogeneity in estimation of local cerebral glucose utilization with current kinetic models of the [^{18}F]fluorodeoxyglucose method. *J Cereb Blood Flow Metab* 12:823–834, 1992
26. Mueckler M: Facilitative glucose transporters. *Eur J Biochem* 219:713–725, 1994
27. Kobayashi M, Nikami H, Morimatsu M, Saito M: Expression and localization of insulin-regulatable glucose transporter (GLUT4) in rat brain. *Neurosci Lett* 213:103–106, 1996
28. Pardridge WM, Eisenberg J, Yang J: Human blood-brain barrier insulin receptor. *J Neurochem* 44:1771–1778, 1985
29. Dringen R, Hamprecht B: Glucose, insulin, and insulin-like growth factor I regulate the glycogen content of astroglia-rich primary cultures. *J Neurochem* 58:511–517, 1992
30. Duckrow RB: Regional cerebral blood flow and glucose utilization during hyperinsulinemia. *Brain Res* 462:363–366, 1988
31. Lucignani G, Namba H, Nehlig A, Porrino LJ, Kennedy C, Sokoloff L: Effects of insulin on local cerebral glucose utilization in the rat. *J Cereb Blood Flow Metab* 7:309–314, 1987
32. Hasselbalch SG, Knudsen GM, Holm S, Hageman LP, Capaldo B, Paulson OB: Transport of D-glucose and 2-fluorodeoxyglucose across the blood-brain barrier in humans. *J Cereb Blood Flow Metab* 16:659–666, 1996
33. Dienel GA, Cruz NF, Mori K, Holden JE, Sokoloff L: Direct measurement of the lambda of the lumped constant of the deoxyglucose method in rat brain: determination of lambda and lumped constant from tissue glucose concentration or equilibrium brain/plasma distribution ratio for methylglucose. *J Cereb Blood Flow Metab* 11:25–34, 1991